Proc. Natl. Acad. Sci. USA
Vol. 83, pp. 6342–6346, September 1986
Biochemistry

Competitive behavior of multiple, discrete B–Z transitions in supercoiled DNA

(B–Z energetics/competing transitions/Z-DNA/topoisomers/statistical mechanics)

RAYMOND J. KELLEHER III, MICHAEL J. ELLISON, PUI S. HO, AND ALEXANDER RICH

Department of Biology, Massachusetts Institute of Technology, Cambridge, MA 02139

Contributed by Alexander Rich, May 13, 1986

ABSTRACT **Conformational transitions in topologically constrained duplex DNA necessarily affect and are affected by other transitional processes throughout the entire molecule. This conformational interdependence of discrete sequences within a given superhelical domain arises through a requisite competition for the free energy of supercoiling. Here we present a generalized statistical mechanical analysis of multiple, competing conformational equilibria in superhelical DNA. This model has been applied, using experimentally determined parameters, to the energetic coupling of two independent B–Z transitions. Specifically, we have monitored the extent of B–Z transition, as a function of negative superhelicity, in topoisomers of a plasmid containing two identical d(C-G)$_n$ inserts using two-dimensional gel electrophoresis. The theoretical results were found to be in good agreement with the experimental data, and we have used this model to predict the competitive behavior of B–Z transitions within sequences differing in length and sequence composition. This competition is shown to have a profound effect upon the B–Z equilibria of those sequences analyzed, resulting in a complex modulation in the extent of Z-DNA formation as a function of negative superhelicity. These theoretical and experimental results show that DNA sequences separated by large distances are capable of communicating structural information.**

In a negatively supercoiled DNA, the topological linking number of the two strands α is lower than that of the theoretically relaxed counterpart α_0^0; this deficit is termed the linking difference ($\alpha - \alpha_0^0$). The stress imposed by altered linkage is distributed linearly between fluctuations in the molecule's duplex twist (*Tw*) and axial writhe (*Wr*) (1, 2):

$$\alpha - \alpha_0^0 = \Delta Tw + \Delta Wr. \quad [1]$$

The resulting torsional and bending deformations may be relieved by local transitions that unwind the molecule. The conversion of right-handed B-DNA to the left-handed Z form is, therefore, a process that is facilitated by negative supercoiling (3–6).

A complete picture of supercoiled DNA necessitates not only an understanding of the structural transitions that may occur, but also a knowledge of the manner in which discrete-local transitions might compete with each other within a given superhelical domain. In a linear or a nicked-circular DNA, the linkage relationship of the two strands need not be constant, and the ability of the strands to swivel removes the barrier to changes in twist. In this context, discrete sequences experience independent conformational equilibria. However, the constancy of the linking number in supercoiled molecules dictates that the free energy of supercoiling maintain a constant value in the absence of strand scission. In this situation, the absorption of undertwist at sites of local transition effectively reduces the free energy available to the remainder of the molecule. As a result, the equilibrium behavior of a segment undergoing conformational transition will depend upon its own sequence composition and length, which determine its energy requirements, as well as the transitional behavior of other sequences within the same topological domain. A complex energetic interplay among sequences susceptible to conformational transition is thus established by topological constraints that fix the linking number.

We have previously used a generalized statistical mechanical treatment to describe the conformational equilibrium of a single Z-forming segment of defined length in negatively supercoiled plasmids (7, 8). In the present work, we extend our statistical mechanical analysis to the competition of multiple, discrete sequences undergoing the B–Z transition in response to negative superhelicity. The competition between cruciform formation and B–Z transition has been considered by Benham (9, 10). The treatment described here is a generalized and quantitative one that utilizes empirical energetic data. We apply this model of competing B–Z transitions to experimental unwinding data derived from a plasmid containing two d(C-G)$_{12}$ segments. In addition, this model is used to predict the competitive behavior of B–Z transitions in several types of sequences contained in the same plasmid, wherein the effects of length and sequence composition on the coupled transitional equilibria are illustrated.

MATERIALS AND METHODS

pDHg16x2, a dimeric version of the plasmid pDHg16 (11), was obtained by purifying the minor dimer component subsequent to gel electrophoresis of the predominantly monomeric form. The dimer was then used to transform *Escherichia coli* strain HB101 and purified by standard methods (12). Topoisomers were prepared for pBR322 and pDHg16x2 by adding various amounts of ethidium bromide to aliquots of plasmid in the presence of topoisomerase I (4). Agarose gel electrophoresis of plasmid topoisomers, gel staining, and photography were performed as reported (7).

RESULTS AND DISCUSSION

Theoretical Treatment of Competing Conformational Transitions. The statistical mechanical analysis of supercoiling-induced structural transition within a single sequence is based upon the zipper model for the helix–coil transition (13, 14), which limits the initiation of transition to a single nucleation event within the chain. The approach, developed by Peck and Wang (15) for the B–Z transition in the homopolymer d(C-G)$_n$, was extended in our previous work to the generalized treatment of transitions within nonhomogeneous sequences

The publication costs of this article were defrayed in part by page charge payment. This article must therefore be hereby marked "*advertisement*" in accordance with 18 U.S.C. §1734 solely to indicate this fact.

Abbreviation: bp, base pair(s).

that preserve the base-pair (bp) interactions of the DNA (7, 8). This statistical mechanical formulation depends on the fact that the linkage deficit of a negatively supercoiled DNA increases the free energy of the molecule relative to the relaxed state, according to the quadratic relationship (16, 17):

$$\Delta G_\tau = K(\alpha - \alpha_0^0)^2, \quad [2]$$

in which K has the value $1100RT/N$ for a DNA greater than 2000 bp in length. This excess free energy may be partitioned between superhelix formation and the stabilization of alternative secondary structures within susceptible sequences. In the present model, local structural transitions are viewed as two-state equilibria, with the B form serving as the reference state. Each possible chain configuration is associated with a free energy change representing the difference between the B form and the transitional state. The unit of propagation in such a model is formally defined as the energetic interaction that is added to the growing chain, in this case the free energy change associated with the dinucleotide.

The distribution of free energy within the molecule is described by the construction of the partition function Q of the system, which is essentially a sum over all possible states of the associated equilibrium constants:

$$Q = \sum_i e^{-(\Delta G_i/RT)}. \quad [3]$$

The probability p_i of a given state is defined in terms of the partition function:

$$p_i = Q^{-1}e^{-(\Delta G_i/RT)}. \quad [4]$$

The average value of some parameter, x, associated with the ith state may then be determined as the product:

$$\langle x_i \rangle = \sum_i x_i p_i. \quad [5]$$

The generalized configuration partition function of the one-chain system is written as the series expansion of terms that distribute the free energy of supercoiling to the stabilization of a chain conformation that alters the twist of the molecule (8):

$$Q = 1 + \sum_{i=1}^{n}\sum_{k=i}^{n} \sigma\left(\prod_{j=i}^{k} s_j\right) e^{-\left(K[\alpha-\alpha_0^0+\left(\sum_{j=i}^{k} a_j\right)+2^b]^2/RT\right)}. \quad [6]$$

Here, σ is the nucleation or cooperativity parameter, which represents the equilibrium constant for the formation of two junctions with unperturbed B-DNA, with a free energy denoted by ΔG_J. The s_j terms represent the contribution to an aggregate equilibrium constant from the transition of the jth dinucleotide; these are derived from the free energy required to stabilize the jth dinucleotide in the alternative conformation (ΔG_{B-Z} for the B–Z transition). The a_j terms represent the degree of unwinding associated with the conversion of the jth dinucleotide from the B form to the conformational alternative. b accounts for the net junctional unwinding occurring at the boundary between B-DNA and the portion of the chain that has undergone conformational conversion (15).

With this model, five parameters are sufficient to evaluate the degree of unwinding resulting from a supercoiling-induced conformational transition that does not disrupt the normal base-pair interactions of the two strands: ΔG_τ, a_j, b, ΔG_J, and ΔG_{B-Z}. The relationship between ΔG_τ and the linking difference has been well established (Eq. 2). By manipulation of the remaining four parameters, this treatment can be applied to a variety of conformational possibilities. Our studies focus on the B–Z transition, for which values have been determined for a_j, b, ΔG_J, and ΔG_{B-Z} for a number of nearest neighbor interactions (7, 8, 15). Implicit in this approach are the assumptions that ΔG_J is sequence independent and that partitioning of ΔG_τ to transitional equilibria elsewhere in the molecule can be neglected.

The only additional assumption necessary to consider the competition of two independent transitions within the same molecule is a fundamental axiom of probability: the frequency of mutual occurrence of two independent events is given by the product of their individual probabilities. On the basis of this precept, the configuration partition function for a system in which two chains of lengths m and n undergo completely independent transitions may be represented as the product of their individual partition functions for a linear DNA molecule:

$$Q = \left(1 + \sum_{i=1}^{n}\sum_{k=i}^{n} \sigma\left(\prod_{j=i}^{k} s_j\right)\right)\left(1 + \sum_{p=1}^{m}\sum_{r=p}^{m} \sigma\left(\prod_{q=p}^{r} s_q\right)\right). \quad [7]$$

However, in a covalently closed circular DNA, the position of the transitional equilibrium of each sequence depends on the stored free energy of supercoiling. Therefore, the transitions of two noncontiguous sequences in a negatively supercoiled DNA occur independently with respect to nucleation and propagation but are interdependent due to the competition for ΔG_τ. The system configuration partition function represents this coupling through the partitioning of the free energy of supercoiling to the stabilization of joint transitional states, with the residual free energy of superhelix formation experiencing the overall reduction in twist from both sequences. In a manner analogous to that employed in the construction of the one-chain partition function for a supercoiled DNA (Eq. 6), each term in the two-chain partition function for a linear DNA, shown in Eq. 7, is combined with an equilibrium constant derived from the residual free energy of superhelix formation so that the total free energy of supercoiling is represented for each state. From this, the expected reduction in twist due to the B–Z transition of both sequences, or of either individual sequence, may be determined as a function of the linking difference. According to Eq. 5, values of $\langle \Delta Tw \rangle$ are calculated as the sum over all states of the product of the change in twist associated with a given state and the probability of that state. It must be emphasized that the quantity of interest in these analyses is the mole, rather than the particle. Thus, the expectation values of $\langle \Delta Tw \rangle$ refer not to a single molecule, but to a molar average.

The approach presented here offers several advantages over the previous theoretical treatments. First, the parameter used to monitor the extent of conformational transition, $\langle \Delta Tw \rangle$, is one that is readily measured experimentally via two-dimensional gel electrophoresis. Second, the variables upon which the evaluation of the partition function and the expectation value of ΔTw depend are aggregate terms whose values can be systematically and accurately determined from experimental data (7, 8, 15). For example, the free energies employed in the evaluation of the partition function represent net values for the nucleation or propagation processes, obviating the need to distinguish among contributions from ionic interactions, stacking and bonding energies, torsional rigidity of the conformational variants, etc. Third, this model has been shown to accurately describe situations in which a single sequence undergoes the B–Z transition within a supercoiled molecule (7, 8, 15). In essence, no further assumptions are involved in its extension to any number of competing transitions.

Application of the Model to Experimental Data. We have applied the statistical mechanical treatment outlined above to the coupling of two discrete B–Z transitions within the same topological domain. The plasmid pDHg16x2, shown in Fig. 1, is a dimer of the 2.2-kilobase plasmid pDHg16, which

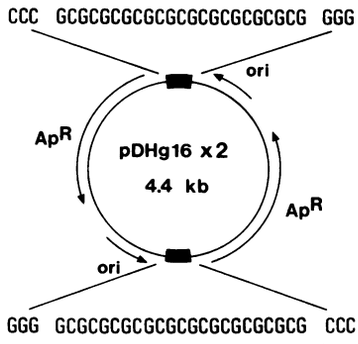

FIG. 1. Plasmid pDHg16x2 is a dimer of pDHg16, a 2.2-kilobase pBR322-derived molecule containing a single insert of 23 bp of $d(C\text{-}G)_n$ in the *Sma* I site. The contribution of the cytosine on the 5′ side of the restriction site increases the effective length of purine-pyrimidine alternation to 24 bp. pDHg16x2, therefore, contains two identical and indistinguishable $d(C\text{-}G)_{12}$ segments.

contains 24-bp of alternating $d(C\text{-}G)_n$ (11). The dimer, therefore, contains two identical and indistinguishable inserts, separated by approximately 2.2 kilobases of duplicate plasmid sequence on either side. The energetic coupling of these sequences may be readily analyzed experimentally using two-dimensional gel electrophoresis, in which a population of topoisomers is separated in two dimensions on the basis of the degree of axial writhe, the property that determines gel mobility. In a given topoisomer, the reduction in twist resulting from B–Z transition is manifested by a corresponding decrease in the magnitude of the writhe component. Topoisomers with linking differences sufficient to induce Z-DNA formation in one or both inserts will, therefore, exhibit retarded mobility in the first dimension. Equilibration of the gel with the intercalator chloroquine shifts the relaxed position, removing any Z-DNA and allowing accurate resolution of topoisomers during electrophoresis in the second dimension. From such an electrophoretic pattern, the extent of B–Z transition may be monitored as a function of the negative linking difference, $-(\alpha - \alpha_0)$ (6, 15).

In Fig. 2 is shown the result of two-dimensional electrophoresis of topoisomers of both pDHg16x2 and the similarly sized plasmid pBR322. Two discrete B–Z transitions become apparent at linking differences of −13.5 and −18.5 in the topoisomer distribution of pDHg16x2. Each transition unwinds the DNA by approximately five turns, a value that agrees with the expected unwinding for the B–Z transition of a segment 24 bp in length. Unwinding data for this plasmid were accumulated from three two-dimensional gels, and a plot of the reduction in twist, $-\langle \Delta Tw \rangle$, as a function of $-(\alpha - \alpha_0)$ gives a biphasic curve in which each phase has a similar transition profile (Fig. 3). For each topoisomer, the $-\langle \Delta Tw \rangle$ value represents the sum of contributions to the net unwinding resulting from transitional states in both segments.

In addition, information regarding the kinetics of the B–Z equilibrium can be obtained from the morphology of topoisomer bands in the two-dimensional separation. The heterogeneity in mobility of each topoisomer is an indication of the variability in the extent of B–Z transition at that value of the linking difference. In Fig. 2*A*, it is apparent that topoisomer bands prior to and subsequent to each B–Z transition display similarly narrow ranges of mobility, suggesting that intermediate kinetic states of the B–Z transition are not discerned to a significant extent. We therefore conclude that the B–Z equilibrium is rapid with respect to the time scale of electrophoresis under these conditions.

The equilibrium statistical mechanical model for the two-chain system may be used to calculate the total theoretical reduction in twist arising from the B–Z transition of these two segments as a function of the linking difference. In assigning values for $\Delta G_{B\text{-}Z}$, the B–Z transition in each segment can be viewed in two ways. First, the formation of Z-DNA can be

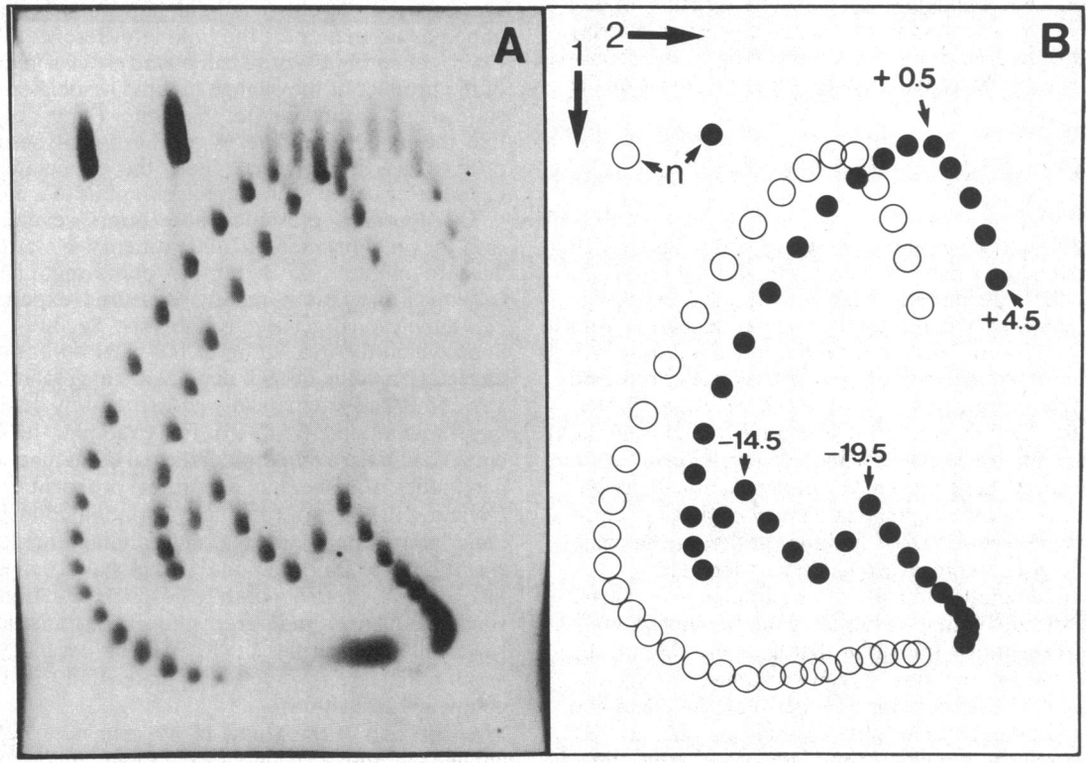

FIG. 2. Two-dimensional gel electrophoresis of topoisomer populations of the control plasmid pBR322 and of the test plasmid pDHg16x2. Photograph of the gel (*A*) and schematic diagram (*B*). *n*, Nicked-circular (form II) plasmid. The negative linking difference, $-(\alpha - \alpha_0)$, of selected topoisomers is indicated. Open circles, pBR322; filled circles, pDHg16x2.

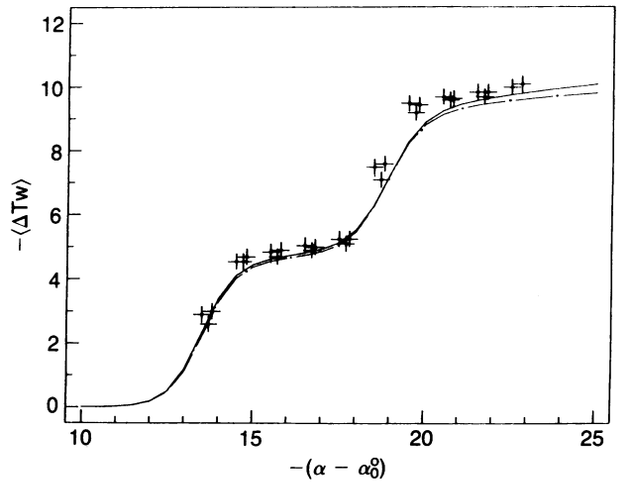

FIG. 3. Application of the statistical mechanical model to experimental data. Here, unwinding data (+) accumulated from two-dimensional electrophoretic separations of topoisomers of pDHg-16x2 are plotted as a function of the negative linking difference, $-(\alpha - \alpha^{\circ}_{\delta})$. Theoretical reduction in twist resulting from the B–Z transition of two competing d(C-G)$_{12}$ segments in a 4380-bp plasmid (dashed lines). Theoretical reduction in twist resulting from the B–Z transition of two competing d[CC(CG)$_{12}$GG] segments in a 4380-bp plasmid (solid lines). The parameters used in the evaluation of $-\langle\Delta Tw\rangle$ have been assigned the values described (7, 15). a_j = −2(1/10.5 + 1/12) turns; b = −0.4 turns; ΔG_J = +5.0 kcal/mol of junction; ΔG_{B-Z} = +0.66 kcal/mol of dinucleotide for the CpG and GpC dinucleotides; ΔG_{B-Z} = +2.4 kcal/mol of dinucleotide for the CpC and GpG dinucleotides. Partition functions and expectation values of ΔTw were evaluated iteratively by numerical analysis using a VAX/VMS 11-780.

limited to the d(C-G)$_{12}$ insert, involving none of the flanking nucleotides of the *Sma* I restriction site (Fig. 1). In this case, only alternating purine-pyrimidine dinucleotides are involved in the propagation of transition, and ΔG_{B-Z} is assigned the value +0.66 kcal/mol of dinucleotide (15). Represented by the broken line in Fig. 3, this treatment is in good agreement with the experimental data.

In the second treatment, the propagation of transition can be viewed as extending into the nucleotides of the *Sma* I site. In this case, the Z-forming sequence is essentially composed of 28 bp of alternating d(C-G)$_n$ with two guanine to cytosine substitutions near the termini. Propagation of the B–Z transition in this sequence will thus additionally involve the nonalternating dinucleotides CpC and GpG, for which ΔG_{B-Z} has been determined to be +2.4 kcal/mol of dinucleotide (7). The expectation values of the reduction in twist calculated for a coupled system consisting of two d[CC(CG)$_{12}$GG] segments are shown as the solid line in Fig. 3. This curve produces a perceptibly better description of the experimental data than the model in which Z-DNA formation is confined to the d(C-G)$_{12}$ portion of the sequence, suggesting that propagation of the transition extends into the flanking sequences. An analysis including additional nucleotides of the flanking regions in the Z-forming segment may, therefore, be in even closer agreement with the experimental data.

It is apparent from Fig. 3 that the molar average reduction in twist in each phase of the transition curve corresponds to that expected for the B–Z transition of the equivalent of one Z-forming segment. In view of the high energetic penalty incurred in the establishment of the B–Z junctions, it is improbable that partially Z-form states will coexist to a significant extent in two segments with energetic identity in the same molecule. Thus, each phase of the observed unwinding represents the complete B–Z transition of one segment within each molecule. Because these segments are energetically identical, one-half of the total population of each segment is involved in each B–Z transition.

A slight but significant discrepancy between the data and both theoretical curves becomes evident in the second transitional phase. This could be due to tertiary structural effects exerted upon regions external to Z-DNA formation. For example, bending or kinking of the DNA as a result of the first B–Z transition could alter the hydrodynamic properties of the molecule in such a way that retarded electrophoretic mobility would not directly correlate with reduced writhing. Such altered mobility would produce a systematic error in the reduction in twist attributed to Z-DNA formation in the second transition.

Predicting the Behavior of Competing B–Z Transitions. The approach presented here may be employed, in combination with the previously determined free energy values for the B–Z transition, to predict the behavior of two competing Z-forming segments within the same superhelical domain. The use of the model for the two-chain system in this capacity is subject to the same restrictions that apply to the one-chain treatment (7). The accuracy of the predictions of the model is limited by the empirical data; the sequences chosen for analysis must be composed of dinucleotide units for which ΔG_{B-Z} values have been experimentally determined.

To examine the effect of sequence length on the competition of two B–Z transitions, we have modeled the transitional behavior of B–Z equilibria in d(C-G)$_{11}$ and d(C-G)$_{12}$ when contained in separate plasmids and in the same plasmid (Fig. 4). The comparison of the uncoupled transitions demonstrates the slightly greater Z-forming propensity of the longer sequence. However, the competition for ΔG_{τ} in the coupled situation produces a striking effect upon the B–Z equilibrium of each sequence: in contrast to the circumstance in which the d(C-G)$_n$ inserts are of identical length, a difference in length of only 8% confers a substantial advantage upon the longer sequence. At a negative linking difference of −17, this is manifested in 3-fold difference in the average extent of Z-DNA formation in the two segment populations.

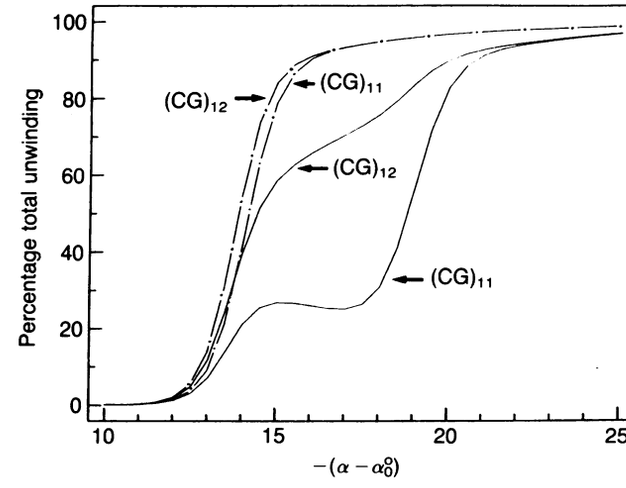

FIG. 4. Prediction of the competitive B–Z transitions of d(C-G)$_{12}$ and d(C-G)$_{11}$. The percentage of the total reduction in twist as a function of negative superhelicity has been calculated for three hypothetical situations from the two-chain partition function described in the text. Predicted extent of Z-DNA formation in each of the sequences d(C-G)$_{12}$ and d(C-G)$_{11}$ undergoing independent, noncompeting B–Z transition in separate superhelical domains 4363 bp in length (equivalent to pBR322) (dashed line). Theoretical B–Z transition curves for the sequences d(C-G)$_{12}$ and d(C-G)$_{11}$ when contained within the same superhelical domain 4363 bp in length (solid line). The relevant parameters have been assigned the values listed in Fig. 3, as determined in previous studies (7, 15).

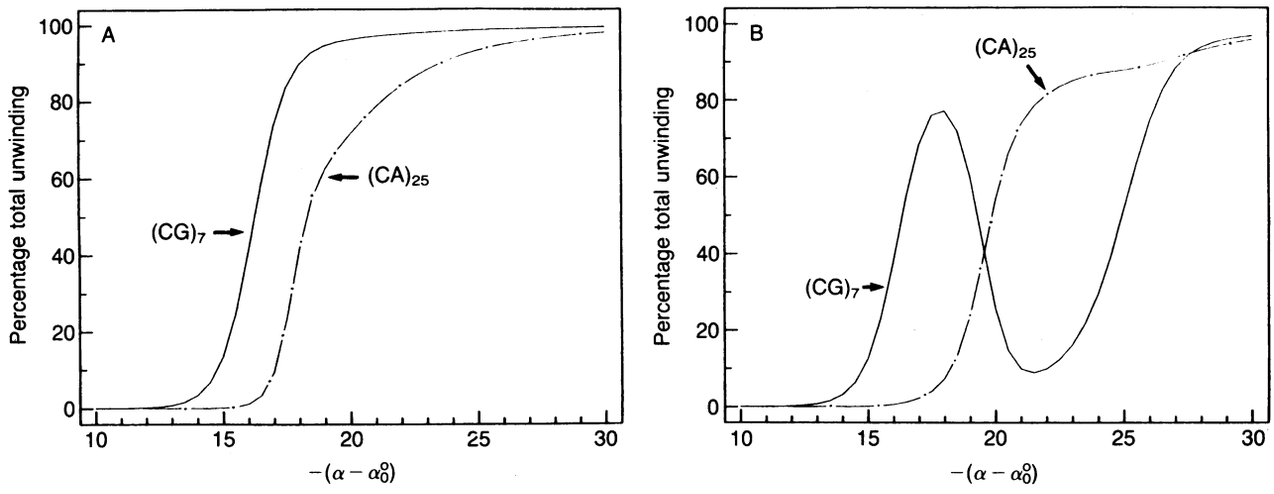

FIG. 5. Prediction of the competing B–Z transitions of $d(C\text{-}G)_7$ and $d(C\text{-}A)_{25}$. (*A*) Expected percentage of the total reduction in twist as a function of the negative linking difference for the sequences $d(C\text{-}G)_7$ and $d(C\text{-}A)_{25}$ when contained as the sole Z-forming segment in a superhelical domain 4363 bp in length. (*B*) Predicted extent of Z-DNA formation in each sequence when both are present within the same superhelical domain 4363 bp in length. These curves were calculated from the two-chain partition function described in the text, with the relevant parameters taking the values listed in Fig. 3, as determined (7, 15). Also, $\Delta G_{B\text{-}Z} = +1.2$ kcal/mol of dinucleotide for the CpA and CpA dinucleotides (6, 18).

The relative effects of sequence composition and sequence length on the distribution of the free energy of supercoiling are illustrated in the competition of B–Z transitions in $d(C\text{-}G)_7$ and $d(C\text{-}A)_{25}$. The extent of Z-DNA formation in each sequence as a function of decreasing linking number is shown for both the uncoupled and coupled equilibria in Fig. 5. It should be noted that the $\Delta G_{B\text{-}Z}$ value assigned to the CpA and ApC dinucleotides was determined from data obtained under slightly different electrophoresis conditions than those employed in the assessment of $\Delta G_{B\text{-}Z}$ values for other dinucleotide units (6, 18). Thus, the accuracy of predictions involving CpA or ApC dinucleotides will depend upon the validity of this value in the context of parameters determined under different conditions. The conformational behavior of the $d(C\text{-}G)_7$ segment is considerably more complex when in the presence of the $d(C\text{-}A)_{25}$ segment. At low values of the negative linking difference, Z-DNA formation is favored in the population of $d(C\text{-}G)_7$ segments. However, at intermediate values of the negative-linking difference, the greater torsional relief afforded by the B–Z transition of the longer $d(C\text{-}A)_{25}$ segment makes this stretch an effective competitor for the free energy of supercoiling, and Z-DNA formation is disfavored in the $d(C\text{-}G)_7$ population. Finally, at high levels of negative superhelicity, the equilibria of both segment populations favor Z-DNA formation.

From these results, it is evident that the energetic competition of multiple, discrete B–Z equilibria in a supercoiled molecule can result in a rather complex variation in the extent of Z-DNA formation as a function of negative superhelicity. This phenomenon is independent of the physical separation of the segments undergoing transition within a given domain; it is due solely to the distribution of a fixed quantity of free energy over that domain as a consequence of topological constraints. The interaction of segments in this way is governed by their sequence composition, which determines the relative energetic requirements, and their length, which determines the energy liberated by the reduction in twist at each value of the linking difference. The modulation in the extent of Z-DNA formation will be most marked when competition occurs between a short segment requiring relatively little energy to effect the B–Z transition, and a longer segment whose energetic needs are significantly greater (Fig. 5).

This treatment of competing B–Z transitions presents a step toward a more quantitative understanding of the intricate processes occurring in supercoiled DNA. Conformational alternatives other than the Z form, which preserve the base-pair interactions of the DNA, can be readily accommodated in this model. Moreover, this approach can also be extended to describe the coupling of transitional equilibria in any number of susceptible segments.

We thank Dr. David Pulleyblank for helpful comments concerning this manuscript. This research was supported by grants from the National Institutes of Health, the American Cancer Society, the National Aeronautics and Space Administration, the Office of Naval Research, and the National Science Foundation. R.J.K. was supported in part by funds from the Undergraduate Research Opportunities Program at the Massachusetts Institute of Technology. M.J.E. was supported by a fellowship from the Medical Research Council of Canada. P.S.H. was supported by a fellowship from the American Cancer Society.

1. Fuller, F. B. (1971) *Proc. Natl. Acad. Sci. USA* **68**, 815–819.
2. Crick, F. H. C. (1976) *Proc. Natl. Acad. Sci. USA* **73**, 2639–2643.
3. Rich, A., Nordheim, A. & Wang, A. H.-J. (1984) *Annu. Rev. Biochem.* **53**, 791–846.
4. Peck, L. J., Nordheim, A., Rich, A. & Wang, J. C. (1982) *Proc. Natl. Acad. Sci. USA* **79**, 4560–4564.
5. Singleton, C. K., Klysik, J., Stirdivant, S. M. & Wells, R. D. (1982) *Nature (London)* **299**, 312–316.
6. Haniford, D. B. & Pulleyblank, D. E. (1983) *Nature (London)* **302**, 632–634.
7. Ellison, M. J., Kelleher, R. J., III, Wang, A. H.-J., Habener, J. F. & Rich, A. (1985) *Proc. Natl. Acad. Sci. USA* **82**, 8320–8324.
8. Ellison, M. J., Feigon, J., Kelleher, R. J., III, Wang, A. H.-J., Habener, J. F. & Rich, A. (1986) *Biochemistry* **25**, 3648–3655.
9. Benham, C. J. (1983) *Cold Spring Harbor Symp. Quant. Biol.* **47**, 219–227.
10. Benham, C. J. (1981) *J. Mol. Biol.* **150**, 43–68.
11. Haniford, D. B. & Pulleyblank, D. E. (1983) *J. Biomol. Struct. Dyn.* **1**, 593–609.
12. Maniatis, T., Fritsch, E. F. & Sambrook, J. (1982) *Molecular Cloning: A Laboratory Manual* (Cold Spring Harbor Laboratory, Cold Spring Harbor, NY).
13. Schellman, J. A. (1958) *J. Phys. Chem.* **62**, 1485–1494.
14. Flory, P. J. & Miller, W. G. (1966) *J. Mol. Biol.* **15**, 284–297.
15. Peck, L. J. & Wang, J. C. (1983) *Proc. Natl. Acad. Sci. USA* **80**, 6206–6210.
16. Depew, R. E. & Wang, J. C. (1975) *Proc. Natl. Acad. Sci. USA* **72**, 4275–4279.
17. Pulleyblank, D. E., Shure, M., Tang, D., Vinograd, J. & Vosberg, H.-P. (1975) *Proc. Natl. Acad. Sci. USA* **72**, 4280–4284.
18. Vologodskii, A. V. & Frank-Kamenetskii, M. D. (1984) *J. Biomol. Struct. Dyn.* **1**, 1325–1333.